ChemComm

Accepted Manuscript

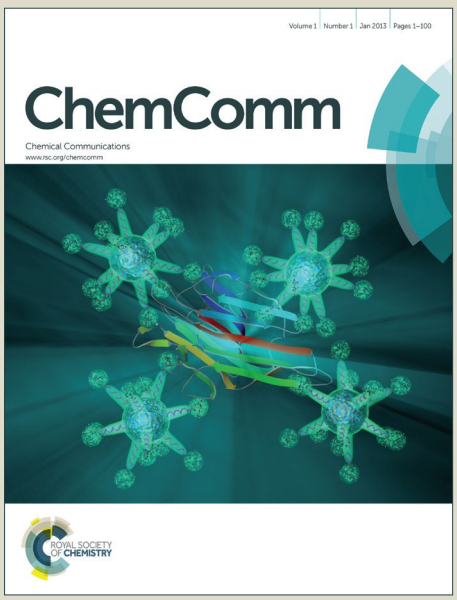

ROYAL SOCIETY OF CHEMISTRY

www.rsc.org/chemcomm

ChemComm

COMMUNICATION

Allosteric stabilization of the amyloid-β peptide hairpin by the fluctuating N-terminal

Received 00th January 20xx,
Accepted 00th January 20xx

DOI: 10.1039/x0xx00000x

www.rsc.org/

Liang Xu[a], Ruth Nussinov[b,c] and Buyong Ma[b]*

Immobilized ions modulate nearby hydrophobic interactions and influence molecular recognition and self-assembly. We simulated disulfide bond-locked double mutants (L17C/L34C) and observed allosteric modulation of the peptide's intra-molecular interactions by the N-terminal tail. We revealed that the non-contacting charged N-terminal residues help the transfer of entropy to the surrounding solvation shell and stabilizing β-hairpin.

Hydrophobic interactions are critical for self-assembly of biomaterial and aggregation-related diseases. Self-assembly of amyloid β (Aβ) monomers into neurotoxic oligomers has been associated with Alzheimer's disease (AD).[1-3] Aβ oligomers are rich in β-sheet conformations, especially β-hairpin structures.[4, 5] Full-length Aβ peptides Aβ(1–40) contain hydrophilic fragment, Aβ(1–16), and Aβ(17–40) which includes two critical hydrophobic patches, residues 17–21 and 30–35.[6] The N-terminal is more soluble and disordered, and is not in the rigid fibril core.[7, 8] Consequently, it is generally regarded redundant in formation of Aβ aggregates and largely neglected in previous investigations.[9] Obviously, without the highly charged N-terminal Aβ(1–16) fragment, Aβ(17–40) would expose more hydrophobic residues to solvent and become less soluble.[10] Aggregation of N-terminal-deleted Aβ such as Aβ(17–40) is highly sensitive to experimental conditions.[11, 12] Both Aβ(17–40) and Aβ(17–42) have lower β-sheet content than the longer Aβ(1–40) and Aβ(1–42) .[11, 12] Mutations in the Aβ N-terminal region (A2V, A2T, H6R, and D7H) affect Aβ aggregation.[13-17] Importantly, both experiment and simulations demonstrated that the distinct changes in aggregation propensity of Aβ mutants are closely related to the alteration of the amount of β-hairpin content.[17-21] Although this highlights the crucial role of Aβ N-terminal region in tuning Aβ assembly, the underlying molecular mechanism has not been elucidated.

The charged residues can strongly modulate nearby hydrophobic interactions,[22] which are the major driving force in amyloid formation.[23-25] However, the allosteric effects of Aβ(1–16) on the intra-molecular interactions of Aβ(1–40) appear more complex than expected earlier. Here we designed simulations to delineate the coupling of the N-terminal and β-sheet forming central region of Aβ(1-40). To enrich the sampling of β-sheet conformations, a disulfide bond was introduced at residues 17/34, as commonly used in stabilizing soluble Aβ peptides to characterize Aβ oligomers experimentally.[26,27] we used extensive replica-exchange molecular dynamics (REMD) simulations of double mutants of Aβ(1–40) (referred to as Aβ(1–40)cc), Aβ(1–34) (Aβ(1–34)cc), and Aβ(17–40) (Aβ(17–40)cc) in explicit solvent to thoroughly explore the interaction of the freely flying N-terminal with other regions (see method in Supplementary Information).

We found that the β-hairpin conformation is stable in both Aβ(1–40)cc and Aβ(1–34)cc but not in Aβ(17–40)cc. **Figure 1** shows representative conformations and their populations of the top five clusters of each ensemble. Compared to the Aβ(17–40)cc, both Aβ(1–40)cc and Aβ(1–34)cc ensembles display higher population of β-hairpin structures. **T**he distribution of the first 100 clusters decreases sharply for each system, suggesting that there is no dominant cluster and different Aβ peptides are still polymorphic due to their disordered nature (Figure S4). The constraint of the disulfide bond does not reduce the conformational diversity, as the top 10 clusters of Aβ(1–40)cc only represent 17.2% of its structure ensemble, less than 36.9% in the top 10 cluster of wild-type Aβ(1–40) as investigated in recent REMD simulations.[28] The result demonstrates that Aβ(17–40)cc becomes more disordered without the Aβ(1–16) fragment although all three peptides are locked by an identical disulfide bond.

Figure 2A shows the distribution of secondary structures of each system. Random coil structures are still dominant, covering 35.2%, 35.8%, and 41.0% of conformations of Aβ(1–40)cc, Aβ(1–34)cc, and Aβ(17–40)cc, respectively. Comparable amounts of bend and turn structures are displayed by each ensemble (38.9%, 38.2%, and 35.4%). The helix content of all

[a] School of Chemistry, Dalian University of Technology, Dalian, China.
[b] Basic Science Program, Leidos Biomedical Research, Inc. Cancer and Inflammation Program, National Cancer Institute, Frederick, MD 21702, USA.
[c] Sackler Inst. of Molecular Medicine Department of Human Genetics and Molecular Medicine Sackler School of Medicine, Tel Aviv University, Tel Aviv 69978, Israel.
*E-mail: mabuyong@mail.nih.gov
† Electronic Supplementary Information (ESI) available: One Table and 10 figures. See DOI: 10.1039/x0xx00000x

structures varies from 5.4% to 7.2%, and the β-sheet contents are 16.4%, 21.7 and 10.0% for the Aβ(1–40)cc, Aβ(1–34)cc, and Aβ(17–40)cc ensembles, respectively (close to the final result of the cumulative average values shown in **Figure S1**). Note that the wild-type Aβ generally exhibits a collapsed coil structure in water.[29] A previous circular dichroism experiment determined that Aβ(1–40) displays 8.7 % α-helix, 24.0% β-sheet, and 67.3% statistical coil.[30] Recent REMD simulations also showed that Aβ(1–40) populates ~25% β-structure, and the most-populated four clusters display β-hairpin motifs.[28] The introduction of a disulfide bond decreases the β-sheet propensity of Aβ(1–40)cc, which is expected because only those conformations that satisfy the constraint imposed by the disulfide bond are able to sample β-sheet conformations.

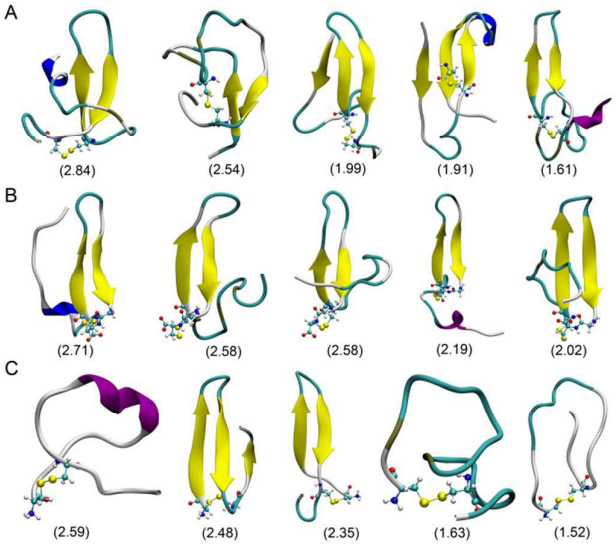

Figure 1. The representative conformations of the top five clusters of conformational ensemble of Aβ(1–40)cc (A), Aβ(1–34)cc (B), and Aβ(17–40)cc (C). The population (%) of each cluster is shown in parentheses.

The per residue secondary structure populations for each Aβcc ensemble were also calculated and shown in **Figure 2**B–2F. Compared with Aβ(1–40)cc, the N-terminal of Aβ(1–34)cc samples less helical structure, whereas Aβ(17–40)cc samples more helical structures in regions involving residues 19–22 and 32–37, and turn structure including residues 19-21 and 28–35. All peptides sample significant β-sheet structures in the 18–22 and 27–32 regions. However, the propensities ranking is Aβ(1–34)cc > Aβ(1–40)cc > Aβ(17–40)cc, indicating that Aβ(17–40)cc samples less β-hairpin conformations. The result is consistent with cluster analysis (**Figure 1**), highlighting the critical role of the N-terminal in stabilizing the β-hairpin structure.

We calculated the contact frequencies to examine how the N-terminal tunes the intra-molecular β-hairpin interactions (**Figure S5**). Significant contacts in the ring region are constrained by the disulfide bond in both Aβ(1–40)cc and Aβ(1–34)cc. These contacts correspond to the interactions in the β-hairpin region. Contacts in other regions are generally less than 20%, which suggests that the intra-molecular interactions between Aβ(1–16) and the rest of the Aβcc are likely transient and allosterically long-range. The SASA values calculated for each residue confirm that there is no stable association between Aβ(1–16) and other regions of Aβcc peptides as each residue in different systems exposes nearly identical surface area (**Figure S6**). However, without the Aβ(1–16) fragment, only weak contacts that potentially sample β-hairpin motif were observed within the ring region in the contact map of Aβ(17–40)cc (**Figures 3** and **S5)**.

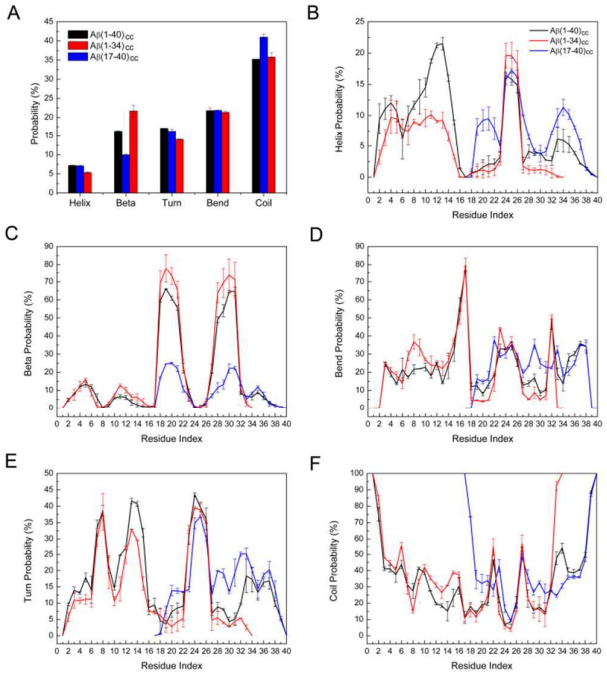

Figure 2. The average percentage of secondary structure calculated for each system. (B-F) The distribution of secondary structures (helix, β-strand, bend, turn, and coil) per residue calculated for each system. The standard deviations were obtained by averaging the results of 100–150 ns and 150–200 ns.

In addition to the β-hairpin regions, more noticeable long range contacts were identified between Aβ(1–16) and the rest of Aβ(1–34)cc/Aβ(1–40)cc when a cutoff of 10 Å was used to define a contact (**Figure S5**). Particularly, in the contact map of Aβ(1–34)cc, discernible contacts (~20%) between Aβ(1–16) and regions containing residues18–20 and 28–32 can be identified (**Figure 3**), suggesting that Aβ(1–16) transiently fluctuates around the β-hairpin region. The orientations of the Aβ(1–16) fragment in Aβ(1–40)cc and Aβ(1–34)cc can be observed in the representative conformations of each cluster as shown in **Figure 1**. To identify the dynamic change of Aβ(1–34)cc and Aβ(17–40)cc with regard to the same region in Aβ(1–40)cc, we calculated the contact difference maps (**Figure 3)**. Without the C-terminal residues 35–40, in addition to the increased contacts in the β-hairpin region, Aβ(1–16) fragment fluctuates more frequently around a wide region involving residues 19–33 in Aβ(1–34)cc than in Aβ(1–40)cc (**Figure 3A**). The N-terminal residues of Aβ(1–34)cc also have long-range contacts, probably because Aβ(1–16) is flexible in aqueous solution. In the absence of residues 1–16, Aβ(17–40)cc displays less frequent contacts in the region locked by the disulfide

bond. Consistently, this closed peptide becomes more disordered than in Aβ(1–40)cc.

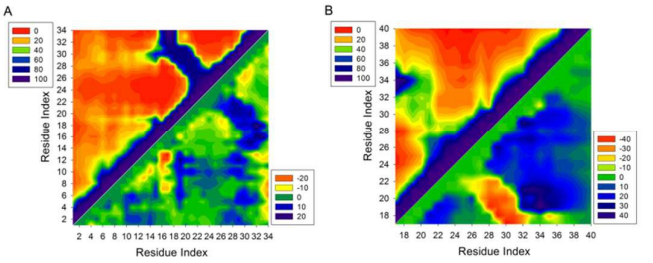

Figure 3. Intra-molecular contact maps. Contact frequencies (%) between amino acids in Aβ(1–34)cc (A) and Aβ(17–40)cc (B). Contact difference maps of Aβ(1–34)cc (A) and Aβ(17–40)cc relative to the contacts between the same amino acids in Aβ(1–40)cc are also shown in the same panel (bottom right). A contact occurs if the center of mass of each residue is within 10 Å of the center of mass of another residue.

Our analyses revealed that the gain of entropy in the N-terminal compensates for the loss of entropy in the β-hairpin. We examined the potential of mean force (PMF) of each system with respect to the two distances between the N- and β-hairpin parts and the number of backbone hydrogen bonds (the Cα atom of Asp[1] and the center of mass of Aβ(17–34) fragment **in Figures 4** and the center of mass of Aβ(1–16) and the center of mass of Aβ(17–34) in **Figure S7**). Both Aβ(1–40)cc and Aβ(1–34)cc display similar free energy landscapes, with the distance restrained to 25 Å and the hydrogen bonds (HB) to a maximum of 16. Only one energy basin was observed in each landscape, corresponding to the most populated distance and number of residues involved in β-hairpin conformation. The energy minimum (ΔG=0 kcal/mol) on each free energy surface suggests that Asp[1] is 13 Å and 15 Å away from the center of the β-hairpin of Aβ(1–40)cc and Aβ(1–34)cc, respectively (**Figure 4**). The most stable conformations of Aβ(1–40)cc and Aβ(1–34)cc involve 11 and 10 backbone HBs. Figure S7 also indicates that when the center of the N-terminal is 10 Å away from the center of the β-hairpin in both systems, the conformations of Aβ(1–40)cc and Aβ(1–34)cc have 10 and 9 HBs in the lowest energy basin. Note that Aβ(1–40)cc can have 18 hydrogen bonds, implying that a total of 9-10 residues could be involved in β-sheet structures. However, although these conformations are accessible, they are not the dominant species with the lowest free energy. Such a result indicates that a balance must be achieved between the gain of enthalpy due to formation of hydrogen bonds and the loss of entropy due to the restriction exerted on the backbone in the extend state of β-sheet conformation. Interestingly, the N-terminal is not fully extended, but moving 10 Å around Aβ(17–34) fragment, partially compensating for the loss of Aβcc entropy.

The movement of water surrounding the peptides reflects the entropy of the solvent environment due to the fluctuations of the N-terminus. To examine the solvent entropy at the room temperature, we performed additional 400-ns simulations for all three peptide systems. We calculated the number of retained water molecules within 10 Å of the Aβ(17–34) motif of each peptide, and summarized the results in Table S1. The number of the retained water molecules between two adjacent trajectories (100 ps) generally decreases throughout the simulations. Although the difference in the number of water molecules over the last 200 ns is only 3–4 for Aβ(1–40)cc and Aβ(17–34)cc, such result indicates that Aβcc could become more disordered and increasingly disrupt the network of water molecules. We observed that the longer the peptides, the lower the number of retained water molecules, suggesting that the dynamics of the terminals can affect the flux of water molecules. The relatively significant decrease in the number of retained water molecules (~15) in the Aβ(17–40)cc system can be attributed to formation of a new β-hairpin structure during 300–400 ns of the simulation, which transfers larger entropy to the surrounding water clusters.

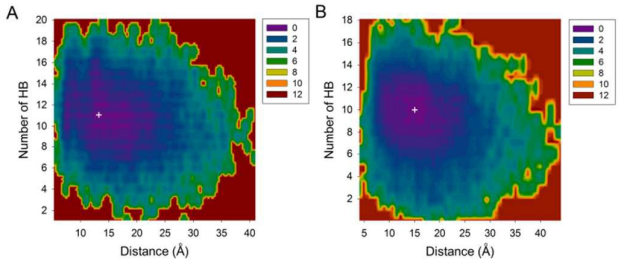

Figure 4. Free energy surface of Aβ(1–40)cc (A) and Aβ(1–34)cc (B) at 310 K in terms of the distance between Cα atom of Asp1 and the center of mass of Aβ(17–34) fragment, and the number of backbone hydrogen bonds (HB) corresponding to the number of residues involving the formation of β-hairpin conformation. The free energy values (in kcal/mol) were obtained by $\Delta G=-kBT(\ln P_i-\ln P_{max})$, where P_i and P_{max} are the probability distributions calculated for specific pairs of distance and number of hydrogen bonds. $\ln P_i-\ln P_{max}$ was used to ensure ΔG=0 for the lowest free energy point (white cross).

Aβ Lys[16] contributes to the stability of β-sheet conformation,[31] and the N-terminal of Aβ can modulate the aggregation rate and fibril stability at low pH,[32] suggesting a synergistic effect of ionic residues: they contribute to the stability of β-sheet conformation and to Aβ peptide assembly. The loss of entropy due to forming β-sheet structures could be compensated by the gain of entropy by the N-terminal, in concert with the charged residues increasing the stability of β-conformations. The free energy change of Aβ(17–34) locked in a β-hairpin conformation is estimated about 9.3 kcal/mol (Supplementary material). Additional entropy is necessary to release the constraints of the locked Aβ(17–34). This entropy compensation can be realized by the movements of the N-terminal residues and solvation water. Aβ(1–16) could become more disordered due to gained entropy. Rebalance of the entropy, as we observed in different Aβcc peptides lengths, could be general in Aβ. For example, the N-terminal of Aβ is the primary metal binding site, and metal binding could decrease entropy and then modulate Aβ self-assembly.[35, 36] Other mechanisms may also operate here, like the change of hydrogen bonding structure of hydration shells,[33] or electric field effects of conformational dynamics and aggregation behavior of peptides.[34]

Aβ peptides are intrinsically unstructured, making it challenging to investigate the effects of the N-terminal on the overall misfolding dynamics. Our simulations of different double mutants L17C/L34C Aβ peptides revealed that Aβ(1–

40)cc samples significant β-hairpin conformations, consistent with experimental findings that this disulfide bond can trap Aβ in β-hairpin structures. Aβ(1–34)cc and Aβ(1–40)cc demonstrate comparable β-hairpin populations, however, the capability of Aβ(17–40)cc to maintain β-hairpin conformation is surprisingly reduced. Aβ(1–16) is more likely to fluctuate around the other region, and modulate the hydrophobic interactions between residues that form β-hairpin conformations. The fluctuations of Aβ(1–16) fragment increases the entropy of both Aβ(1–40)cc and Aβ(1–34)cc and solvation water molecules, which in turn helps to stabilize the β-hairpin structures. In the absence of this part, Aβ(17–40)cc becomes more disordered and populates less β-hairpin conformations. Our study clearly demonstrated that the fluctuating N-terminal allosterically enhances the β-hairpin stability of the amyloid β peptide in the central amyloidogenic region. While the N-terminal residues can transiently interact with the central regions of Aβ(1–40) through hydrophobic interactions and hydrogen bonding, the most favored distance between the N-terminal fragment and central region is around 10 Å. We found that the transfer of entropy to the surrounding solvation shell is connected to the stabilization of the β-hairpin, helped by nearby fluctuating charged N-terminal residues. Our work provides strong support and explanation to recently observed effects that immobilized charged residues can modulate nearby hydrophobic interactions. The function of entropy compensation in concert with charged residues within Aβ peptides may be a general mechanism regulating the dynamics along misfolding and aggregation pathways.

This work was supported by NIH contract number HHSN261200800001E. This research was supported (in part) by the Intramural Research Program of the CCR, NCI, NIH. Xu thanks China Scholarship Council (CSC201306065001). MD simulations were performed at the Biowulf PC/Linux cluster at the NIH (http://biowulf.nih.gov/).

Notes and References

1. R. Kayed and C. A. Lasagna-Reeves, *J Alzheimers Dis*, 2013, **33 Suppl 1**, S67-78.
2. I. Benilova, E. Karran and B. De Strooper, *Nature Neuroscience*, 2012, **15**, 349-357.
3. A. Laganowsky, C. Liu, M. R. Sawaya, J. P. Whitelegge, J. Park, M. Zhao, A. Pensalfini, A. B. Soriaga, M. Landau, P. K. Teng*, et al.*, *Science*, 2012, **335**, 1228-1231.
4. T. P. J. Knowles, M. Vendruscolo and C. M. Dobson, *Nature Reviews Molecular Cell Biology*, 2014, **15**, 384-396.
5. M. Ahmed, J. Davis, D. Aucoin, T. Sato, S. Ahuja, S. Aimoto, J. I. Elliott, W. E. Van Nostrand and S. O. Smith, *Nature Structural & Molecular Biology*, 2010, **17**, 561-567.
6. R. Liu, C. McAllister, Y. Lyubchenko and M. R. Sierks, *Journal of Neuroscience Research*, 2004, **75**, 162-171.
7. A. T. Petkova, Y. Ishii, J. J. Balbach, O. N. Antzutkin, R. D. Leapman, F. Delaglio and R. Tycko, *Proceedings of the National Academy of Sciences*, 2002, **99**, 16742-16747.
8. T. Luhrs, C. Ritter, M. Adrian, D. Riek-Loher, B. Bohrmann, H. Dobeli, D. Schubert and R. Riek, *Proceedings of the National Academy of Sciences*, 2005, **102**, 17342-17347.
9. J. Nasica-Labouze, P. H. Nguyen, F. Sterpone, O. Berthoumieu, N.-V. Buchete, S. Coté, A. De Simone, A. J. Doig, P. Faller, A. Garcia*, et al.*, *Chemical Reviews*, 2015, **115**, 3518-3563.
10. F. Dulin, F. Léveillé, J. B. Ortega, J.-P. Mornon, A. Buisson, I. Callebaut and N. Colloc'h, *FEBS Letters*, 2008, **582**, 1865-1870.
11. C. J. Pike, M. J. Overman and C. W. Cotman, *Journal of Biological Chemistry*, 1995, **270**, 23895-23898.
12. A. Vandersteen, E. Hubin, R. Sarroukh, G. De Baets, J. Schymkowitz, F. Rousseau, V. Subramaniam, V. Raussens, H. Wenschuh, D. Wildemann*, et al.*, *FEBS Letters*, 2012, **586**, 4088-4093.
13. M. Messa, L. Colombo, E. del Favero, L. Cantu, T. Stoilova, A. Cagnotto, A. Rossi, M. Morbin, G. Di Fede, F. Tagliavini*, et al.*, *J Biol Chem*, 2014, **289**, 24143-24152.
14. I. Benilova, R. Gallardo, A. A. Ungureanu, V. Castillo Cano, A. Snellinx, M. Ramakers, C. Bartic, F. Rousseau, J. Schymkowitz and B. De Strooper, *J Biol Chem*, 2014, **289**, 30977-30989.
15. P. Das, B. Murray and G. Belfort, *Biophysical Journal*, 2015, **108**, 738-747.
16. A. I. Bush, W.-T. Chen, C.-J. Hong, Y.-T. Lin, W.-H. Chang, H.-T. Huang, J.-Y. Liao, Y.-J. Chang, Y.-F. Hsieh, C.-Y. Cheng*, et al.*, *PLoS ONE*, 2012, **7**, e35807.
17. K. Ono, M. M. Condron and D. B. Teplow, *Journal of Biological Chemistry*, 2010, **285**, 23186-23197.
18. M. H. Viet, P. H. Nguyen, S. T. Ngo, M. S. Li and P. Derreumaux, *ACS Chemical Neuroscience*, 2013, **4**, 1446-1457.
19. M. H. Viet, P. H. Nguyen, P. Derreumaux and M. S. Li, *ACS Chemical Neuroscience*, 2014, **5**, 646-657.
20. P. M. Truong, M. H. Viet, P. H. Nguyen, C.-K. Hu and M. S. Li, *The Journal of Physical Chemistry B*, 2014, **118**, 8972-8981.
21. L. Xu, Y. Chen and X. Wang, *Proteins: Structure, Function, and Bioinformatics*, 2014, **82**, 3286-3297.
22. C. D. Ma, C. Wang, C. Acevedo-Vélez, S. H. Gellman and N. L. Abbott, *Nature*, 2015, **517**, 347-350.
23. S. H. Chong and S. Ham, *Proceedings of the National Academy of Sciences*, 2012, **109**, 7636-7641.
24. Y. Luo, P. Dinkel, X. Yu, M. Margittai, J. Zheng, R. Nussinov, G. Wei and B. Ma, *Chem Commun (Camb)*, 2013, **49**, 3582-3584.
25. B. Ma and R. Nussinov, *Curr Opin Chem Biol*, 2006, **10**, 445-452.
26. L. Yu, R. Edalji, J. E. Harlan, T. F. Holzman, A. P. Lopez, B. Labkovsky, H. Hillen, S. Barghorn, U. Ebert, P. L. Richardson*, et al.*, *Biochemistry*, 2009, **48**, 1870-1877.
27. T. Härd, *FEBS Journal*, 2011, **278**, 3884-3892.
28. D. J. Rosenman, C. R. Connors, W. Chen, C. Wang and A. E. García, *Journal of Molecular Biology*, 2013, **425**, 3338-3359.
29. S. Zhang, K. Iwata, M. J. Lachenmann, J. W. Peng, S. Li, E. R. Stimson, Y. Lu, A. M. Felix, J. E. Maggio and J. P. Lee, *J Struct Biol*, 2000, **130**, 130-141.
30. K. Ono, M. M. Condron and D. B. Teplow, *Proceedings of the National Academy of Sciences*, 2009, **106**, 14745-14750.
31. P. E. Fraser, D. R. McLachlan, W. K. Surewicz, C. A. Mizzen, A. D. Snow, J. T. Nguyen and D. A. Kirschner, *J Mol Biol*, 1994, **244**, 64-73.
32. K. Brännström, A. Öhman, L. Nilsson, M. Pihl, L. Sandblad and A. Olofsson, *Journal of the American Chemical Society*, 2014, **136**, 10956-10964.
33. P. K. Verma, H. Lee, J.-Y. Park, J.-H. Lim, M. Maj, J.-H. Choi, K.-W. Kwak and M. Cho, *The Journal of Physical Chemistry Letters*, 2015, **6**, 2773-2779.
34. C. M. Kelly, T. Northey, K. Ryan, B. R. Brooks, A. L. Kholkin, B. J. Rodriguez and N. V. Buchete, *Biophysical chemistry*, 2015, **196**, 16-24.
35. Y. Miller, B. Ma and R. Nussinov, *Proc Natl Acad Sci U S A*, 2010, **107**, 9490-9495.
36. L. Xu, S. Shan, Y. Chen, X. Wang, R. Nussinov and B. Ma, *Journal of chemical information and modeling*, 2015, **55**, 1218-1230.

Table of contents entry:

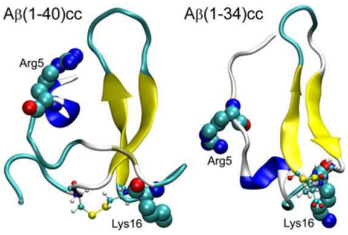

Fluctuating N-terminal allosterically stabilize amyloid-β peptide hairpin by dissipating entropy into solvent.